



Experimental Investigation of Pressure Drop with Particle Loading in Nuclepore Filters

*Constantinos Sioutas, Petros Koutrakis, Pen-Yau Wang,
Peter Babich, and Jack M. Wolfson*

UNIVERSITY OF SOUTHERN CALIFORNIA, DEPARTMENT OF CIVIL ENGINEERING,
LOS ANGELES, CA 90089 (C. S.), HARVARD UNIVERSITY, SCHOOL OF PUBLIC HEALTH,
DEPARTMENT OF ENVIRONMENTAL HEALTH, BOSTON, MA 02115
(P. K., P.-Y. W., P. B., J. M. W.)

ABSTRACT. This paper presents an experimental investigation of the increase in pressure drop with particle loading in Nuclepore filters. The average increase in pressure drop per unit time and particle mass concentration was measured as a function of particle size, density, and hygroscopicity. Two different Nuclepore filter pore diameters were tested (2 and 5 μm , respectively) at filter face velocities ranging from 4 to 52 cm/s.

Our results showed that the increase in the pressure drop with particle loading inversely proportional to the square root of particle specific gravity and depends weakly on particle diameter (to the power of -0.2). Furthermore, the increase in the pressure drop with particle loading is proportional to the filter face velocity and inversely proportional to the cube of the pore diameter. Particle interception and impaction on the pore edges are the main deposition mechanisms that are responsible for raising the pressure drop over time across the filter, especially for particles having Stokes numbers below 5. Particle deposition due to diffusion inside the pores is important for particles smaller than 0.2 μm . These observations agree well with previously published studies on particle deposition on the pore edges in Nuclepore filters. Our tests also showed a dramatic decrease in the pressure drop with loading for hygroscopic particles as the relative humidity increases from 10% to 50%. The pressure drop with loading decreases almost inversely proportional to the relative humidity for ammonium sulfate particles.

INTRODUCTION

Over the past two decades, several investigators have examined the pressure drop in filters as a function of particle loading (Spurny et al. 1969; Novick et al. 1992; Gupta et al. 1994; Japuntich et al. 1997). Regardless of the type of filter used to collect particles, these investigations showed that the pressure drop increases linearly with particle loading in the beginning, and af-

ter a certain amount of particles have deposited on the filter, that increase becomes exponential. Other factors affecting the relationship between pressure drop and particle loading include particle diameter, relative humidity, and particle hygroscopicity.

In the past three years, we have attempted to develop a continuous particle mass monitor. This method is based on the measurement of

the increase in the pressure drop with particle loading across porous membrane filters (Nuclepore) over time (Koutrakis et al. 1995; Wang 1997). As part of this development, we investigated both experimentally and theoretically the effect of parameters such as particle size, chemical composition, filter face velocity, and pore size, on the increase in the pressure drop with particle loading. In this article, we describe the results of these investigations.

BACKGROUND

Nuclepore Filters

Nuclepore filters are thin (6–12 μm) nonhygroscopic polycarbonate membranes with circular pores normal to the surface. The theoretical prediction for the particle collection efficiency of these filters has been based on models that assumed uniformly distributed arrays of equal size pores (Pich 1964; Spurny et al. 1969a). The main mechanisms affecting particle capture are:

1. impaction of large particles on the filter surface due to deflection of the air streamlines;
2. interception of particles whose size is comparable to the pore size;
3. diffusion of small particles to the pore walls;
4. retention of particles larger than the pores (sieve effect); and
5. electrostatic effects.

Electrostatic effect is the only mechanism that has not been thoroughly studied, but it has been considered insignificant compared to the rest of the collection mechanisms.

The pressure drop across Nuclepore filters as a function of mass loading for particles of different sizes has not been studied as extensively. Spurny et al. (1969b and 1974) studied the time development of pressure drop in Nuclepore filters in an attempt to understand clogging mechanisms. Three different clogging stages were identified. In the first stage, pressure drop increases gradually with time due to the decrease in the pore size caused by particle deposition. In

the second stage, a complete filling of the pores occurs that is accompanied by a sharp increase in the pressure drop. In the final stage, air is filtered through heaps of particles and since the thickness of this particulate plug grows slowly, the pressure drop increases more slowly. A theoretical model was developed to predict the pressure drop as a function of particle and filter parameters. The Hagen-Poiseuille equation was used to express the pressure drop in the form:

$$\Delta P = \frac{128\mu LQ}{\pi D_t^4 N_f} \quad (1)$$

where N_f is the number of pores, Q the total flow rate, L the pore length (i.e., filter thickness), and D_t the effective pore size, which was assumed to be a function of time. The authors assumed that the effective pore size is decreased with time due to particle loading as follows:

$$\frac{\pi}{4} D_t^2 = \frac{\pi}{4} D_0^2 - \frac{\pi}{6} d_p^3 n_0 \frac{Ut}{LN_0} f \eta \quad (2)$$

where N_0 is the number of pores per unit filter area, n_0 the particle number concentration, L the pore length, D the initial pore size, t sampling duration, η the fraction of particles depositing inside the filter, U the filter face velocity, and f an empirical factor that is equal to 1 for liquid particles and:

$$f = \frac{3}{2} \frac{D}{D + \left(\frac{d_p}{D}\right)^{0.43}} \quad (3)$$

for solid particles. The empirically-based correction for solid particles was made to account for the fact that, unlike liquid particles, solid particles do not coat the pore wall uniformly upon deposition, thus influencing the particle layer thickness and geometry. Equation (1) considers only the pressure drop due to viscous flow inside the pore (frictional loss), which accounts for the majority of the pressure drop across the Nuclepore filter, but ignores pressure losses due to flow entering and exiting the pore. Furthermore, Equation (1) assumes

that all particles collected by the filter are responsible for raising the pressure drop across it. Nevertheless, a particle collected due to impaction onto the area between the pores of the filter cannot increase the pressure drop through the filter. Only particles depositing inside the pores or on the edge of the pores are responsible for raising the pressure drop with particle loading through the Nuclepore filter. Although the expression by Spurny et al. (1969a) is probably correct for particles depositing due to diffusion inside the pore, it cannot be readily applied to the case of particles depositing on the pore due to combined interception/impaction. Consequently, we decided to first determine experimentally the effect of parameters such as particle size and density, as well as filter face velocity and pore size on the pressure drop with loading. Based on the results from these experiments, we then developed predictive models describing the functional relationship between the increase in pressure drop with loading and the aforementioned parameters.

EXPERIMENTAL

The relationship between pressure drop across the particle-sampling Nuclepore filter per unit time as a function of particle concentration and size was investigated for various pore diameters and sampling flow rates. We tested two different pore size Nuclepore filters whose characteristics are shown in Table 1. In addition, the experimental parameters are summarized in Table 2.

The experimental setup is shown in Figure 1. This system consists of four major components:

TABLE 2. Summary of the experimental parameters.

Particle size range (μm)	0.05–3.0
Particle density range (g/cm^3)	1.05–2.2
Filter face velocity (cm/s)	4–52
Relative humidity (%)	10–60
Nuclepore pore size (μm)	2.0 and 5.0

1. the particle generation system that produces mono or polydispersed particles under controlled relative humidity (RH);
2. the particle distributor that supplies particles to each sampling port;
3. a collection unit that includes filters, transducers, and a RH/Temperature sensor; and
4. the signal processing unit.

Suspensions of monodisperse fluorescent yellow-green latex microspheres (Fluoresbrite, Polysciences, Warrington, PA), as well as polydisperse ammonium sulfate, sodium chloride, and potassium nitrate aerosols were nebulized by a pocket nebulizer (Retec X-70/N) using room air at 20 psi. Particle size ranged from 0.05 to $2.7 \mu\text{m}$. The volumetric flow rate of the nebulizer was estimated to be approximately 5.5 LPM and the output was approximately $0.25 \text{ cm}^3/\text{min}$ of fluorescent suspension. The nebulizer was connected to a syringe pump in order to atomize large amounts (120 mL) of the fluorescent suspension. In addition, the output of the nebulizer was maintained constant to ensure a stable atomization process. The generated aerosol was drawn through a 1-liter cylindrical chamber where ten Polonium 210 ionizing units were placed (Staticmaster, NRD Inc.) to

TABLE 1. Specifications of Nuclepore polycarbonate filters tested.

Pore Size (μm)	Pore density (pores/ cm^2)	Nominal Thickness (μm)	Typical Air Flow for Air at 10 psi* (L/min/ cm^2)	Porosity
2	2×10^6	10	65	0.063
5	4×10^5	10	55	0.10

* 10 psi the pressure drop across the unloaded filter.

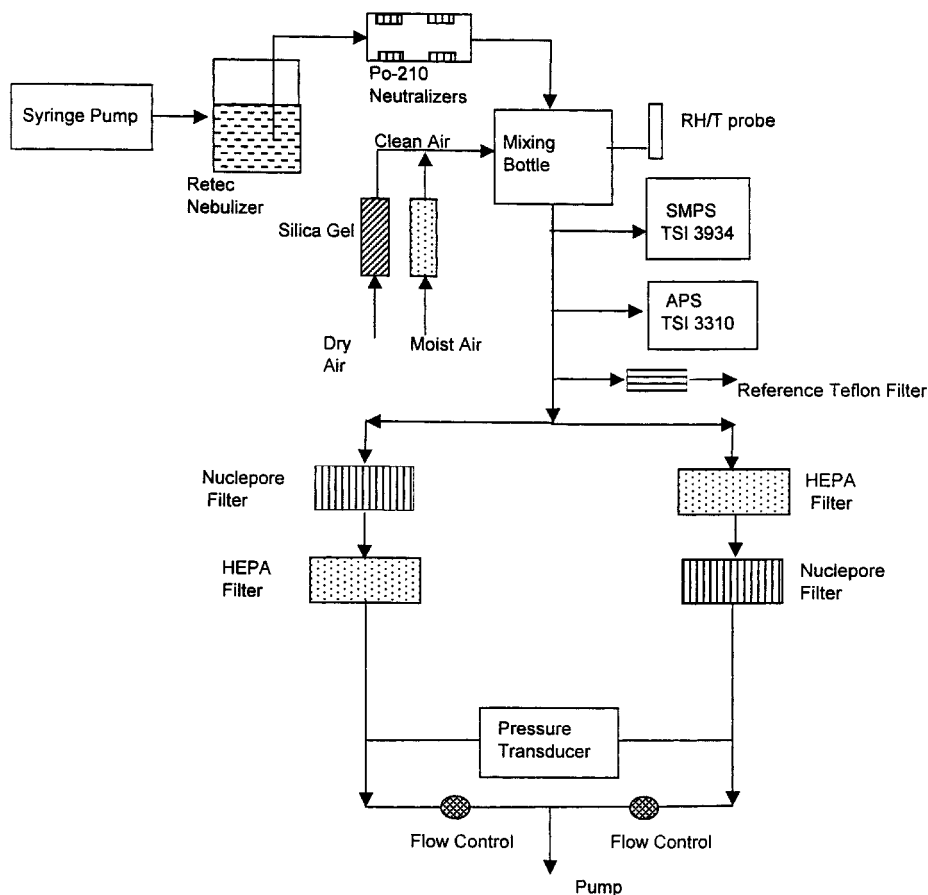


FIGURE 1. Schematic of the test apparatus used for measuring the pressure drop with particle loading in Nuclepore filters.

reduce electrostatic charges carried by the generated particles to the Boltzmann equilibrium. Subsequently, the aerosol was mixed with clean (particle-free) air with controlled RH. RH was controlled by adjusting the flow rates of a dry and a moist airstream, as shown in Figure 1. After the mixing chamber, the aerosol was then drawn through a distributor with a RH/Temperature probe connected to it; part of the aerosol was drawn through a control Teflon filter, used as a reference, to determine the mass concentration of the input aerosol. The test sample was drawn through a Nuclepore filter followed by a HEPA filter. For the reference pressure drop compo-

nent, particle-free air was provided by pumping another portion of the sample air through an absolute filter (HEPA filter, Millipore Corp., Bedford, MA). This clean air was produced in excess of the flow for the pressure drop measurement. Fine adjustment of the clean air flow was used for initial matching of pressure drops for the test and reference Nuclepore filters.

Both particle and clean air sampling Nuclepore filters were sampling at the same flow rate. The pressure difference downstream the two Nuclepore filters was continuously monitored with a transducer connected to a recorder (0–2" H₂O range, Model PX653-02D5V, Omega Engineer-

ing Inc., Stamford, CT). The relative humidity and temperature of the sampled aerosol were also monitored continuously throughout the experimental tests. Aerosol mass concentrations ranged from 5 to 80 $\mu\text{g}/\text{m}^3$.

In order to investigate the effect of particle density (or equivalently, specific gravity), particles with different densities were used: polydisperse potassium carbonate ($\rho_p = 2.3 \text{ g}/\text{cm}^3$), sodium chloride ($\rho_p = 1.9 \text{ g}/\text{cm}^3$), and ammonium sulfate ($\rho_p = 1.7 \text{ g}/\text{cm}^3$), as well as monodisperse silica beads ($\rho_p = 2.2 \text{ g}/\text{cm}^3$, Bangs Laboratories, Inc., Carmel, IN). Each compound was tested in two concentration ranges: 10 to 20 $\mu\text{g}/\text{m}^3$, and 40 to 60 $\mu\text{g}/\text{m}^3$. All tests were performed under controlled RH and temperature conditions (RH = 35–40%, and $T = 20\text{--}22^\circ\text{C}$). In every experiment, the size distribution of particles smaller than 0.7 μm was measured using a TSI Scanning Particle Mobility Analyzer (SMPS 3934, TSI Inc., St. Paul, MN), whereas the size distribution of particles larger than 0.7 μm was monitored using an Aerodynamic Particle Sizer (APS 3310, TSI Inc., St. Paul, MN).

Previous studies by Gupta et al. (1993) demonstrated a strong dependence of the pressure drop in fibrous filters on the relative humidity, especially for hygroscopic particles. To further this investigation to Nuclepore filters, we generated polydisperse ammonium sulfate aerosols (as described in the previous paragraph) and varied the relative humidity of aerosol from 10 to 60%.

RESULTS AND DISCUSSION

Effect of Particle Size

For each experiment, the total increase in the pressure drop across the filter in one hour was divided by the mass concentration measured with the reference filter gravimetrically. This new variable, $d(\Delta P)/c_m/t$ was plotted as a function of particle diameter. Results from the experimental measurements of the pressure drop per

unit time and mass concentration are shown in Figures 2 and 3.

Figure 2 shows the average increase in pressure drop per unit time and mass concentration, $d(\Delta P)/c_m/t$, expressed in $\text{dyn}/\text{cm}^2/\text{s}$ per $\mu\text{g}/\text{m}^3$, for particles of different sizes and for different face velocities for a 5 μm pore filter, whereas Figure 3 shows the average pressure drop per unit time and mass concentration for a 2 μm pore filter.

The results shown in Figures 2 and 3 show similar trends on the dependence of the parameter $d(\Delta P)/c_m/t$ on particle size. In general, $d(\Delta P)/c_m/t$ decreases slightly with particle size for particles from about 0.2 to 1.0 μm for any pore size and face velocity. There is a sharp increase in $d(\Delta P)/c_m/t$ as particle size becomes smaller than 0.2 μm , and with the slope becoming about 30–50% higher than the 0.2–1.0 μm average at about 0.1 μm , and nearly doubling at 0.05 μm . Furthermore, depending on the filter face velocity, the value of $d(\Delta P)/c_m/t$ decreases sharply for the larger particles. At higher filter face velocities (i.e., 12 cm/s or higher) the decrease in $d(\Delta P)/c_m/t$ starts at about 1.0 μm .

The sharp decrease in $d(\Delta P)/c_m/t$ for particles larger than 1.0 μm is due to impaction of these particles on the interpore surfaces of the Nuclepore filter. As these particles do not obstruct the flow through the filter pores, they do not contribute to the increase in the pressure drop with loading. This phenomenon becomes particularly pronounced at higher filter face velocities, as expected.

Several studies investigated particle deposition on a sharp contraction (like that of the flow entering the pore of the Nuclepore) due to combined impaction/interception (Ye and Pui 1990; Muyschondt et al. 1996; Manton 1978; Fan et al. 1978). The theoretical analyses conducted by Ye and Pui (1990) and by Muyschondt et al. (1996) and on particle deposition in abrupt tube contractions showed a very strong dependence of the deposition efficiency on the square root of particle Stokes number, which includes the

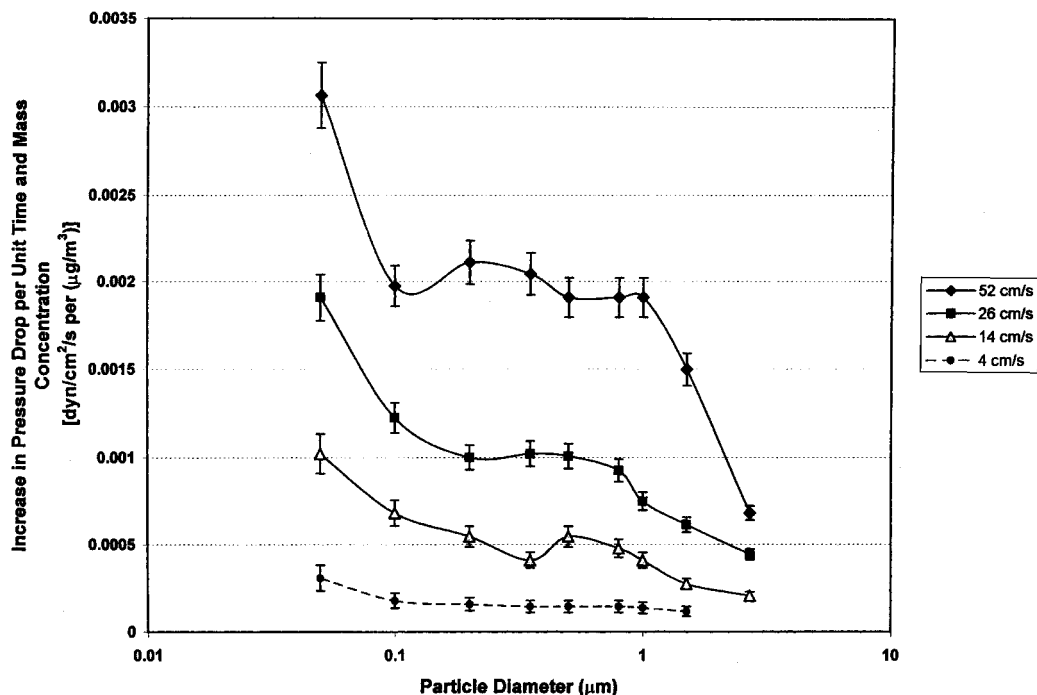


FIGURE 2. Pressure drop with particle loading for a 5- μ m Nuclepore filter as a function of particle size and filter face velocity. Tests were conducted using monodisperse polystyrene latex particles.

Cunningham slip correction factor. Unfortunately, the expressions derived in these studies include both particles depositing on the edge of the contraction as well as the solid surface around the contraction. Thus, they cannot be readily used to predict particle deposition on the edge of Nuclepore filters due to combined interception/impaction.

A rigorous expression, taking into account the combined effects of impaction and interception, was derived by Smith and Phillips (1975) by solving the Navier-Stokes equations of a viscous flow to a circular aperture and determining particle trajectories as a function of Stokes numbers (St_f). The Stokes number, St_f , is defined as:

$$St_f = \frac{\rho_p C_c U d_p^2}{9\mu p D} \quad (4)$$

where d_p is the particle diameter, U the face velocity at the filter, C_c the Cunningham slip

correction, μ the viscosity of the air, D the diameter of the pores, p the filter porosity, and ρ_p the density of the particles. The study showed that particles having $St_f > 5$ impact mostly on the solid surfaces of the filter. For those St_f , the collection efficiency curve resembles that of a conventional impactor. Particles with $St_f < 5$ impact either on the pore edge or penetrate the pore. Particle collection efficiency was expressed in terms of the ratio d_a/D , where d_a is the aerodynamic particle diameter.

For $0.02 < d_a/D < 0.8$, and $St_f < 5$, the collection efficiency due to this combined impaction/interception onto the pore edges was approximated by a linear relationship (correlation coefficient $R^2 = 0.97$) in the following form:

$$\eta_{IR} = K_1 \frac{d_a}{D} = K_1 \frac{\sqrt{\rho_p} d_p}{D} \quad (5)$$

where the dimensionless constant K_1 typically takes values in the range 1.1–1.2.

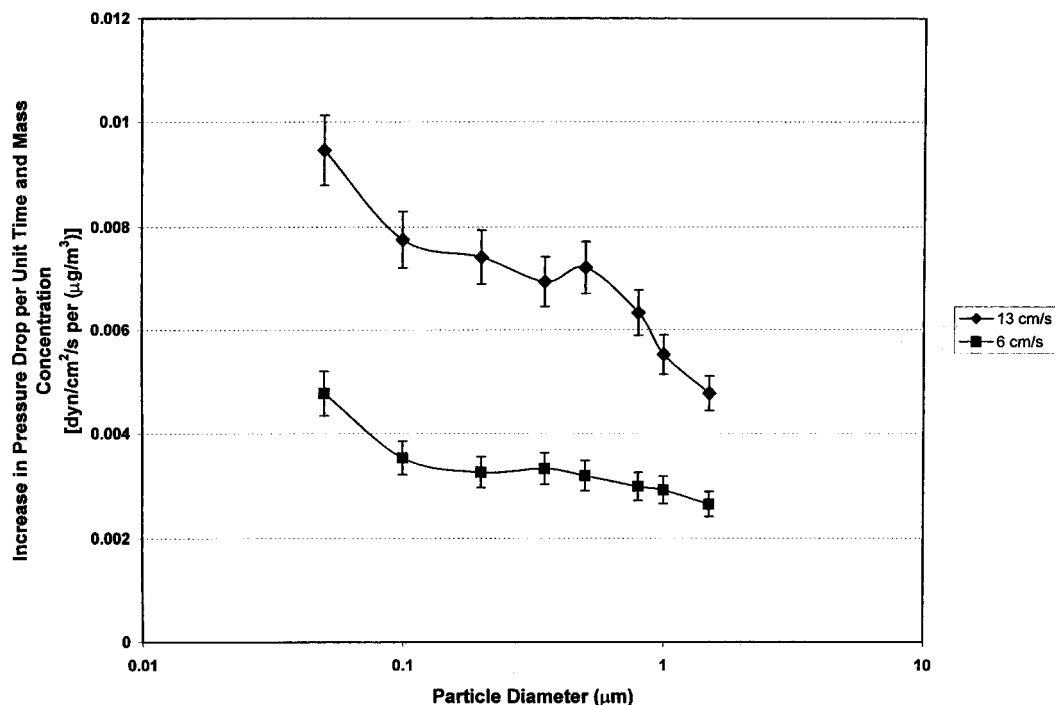


FIGURE 3. Pressure drop with particle loading for a 2- μ m Nuclepore filter as a function of particle size and filter face velocity. Tests were conducted using monodisperse polystyrene latex particles.

As it can be seen in Figure 2, there is no detectable decrease in $d(\Delta P)/c_m/t$ at a face velocity of 4 cm/s. At a face velocity of 13 cm/s and 26 cm/s, the first noticeable decrease is observed for a particle size of 2 μ m (the corresponding Stokes numbers are 5.9 and 11.8, respectively), whereas at 52 cm/s the value of $d(\Delta P)/c_m/t$ decreases sharply at 1 μ m (the corresponding $St_f = 6.4$). For particles having Stokes numbers smaller than a value of about 5, the slope remains practically unaltered until particle size becomes smaller than about 0.2 μ m. In order to confirm the independence of $d(\Delta P)/c_m/t$ on particle diameter for particles in the range 0.2–1.0 μ m, linear regression of $d(\Delta P)/c_m/t$ on particle diameter was performed for each filter face velocity and pore diameter. The increase in pressure drop per unit time and mass concentration was therefore ex-

pressed as follows:

$$\frac{d(\Delta P)}{c_m t} = A_0 + x_1 d_p \quad (6)$$

In Equation (6) $d(\Delta P)/c_m/t$ and A_0 are expressed in $\text{dyn/cm}^2/\text{s}$ per $\mu\text{g/m}^3$ and d_p in μm .

Results of this regression are summarized in Table 3. For each face velocity and pore size, the values of constants A_0 and x_1 , along with their corresponding p -values are presented. The results of Table 3 clearly show that x_1 (i.e., the slope of the regression line) for each configuration is statistically not different from zero, thereby indicating that $d(\Delta P)/c_m/t$ is independent of particle size for particles in the size range of 0.2–1.0 μ m. The value of A_0 represents the average increase in pressure drop per unit time and mass concentration for each configuration for particles in the size ranges 0.2–1.0 μ m.

TABLE 3. Summary of the linear regression of the increase in pressure drop per unit time and particle concentration on particle diameter (d_p), for each filter face velocity (U), and filter pore diameter (D). The regression is performed only for particles in the size range of 0.2–1.0 μm .

Filter Pore Diameter (μm)	Face Velocity (cm/s)	Constant (A_0) (dyn/cm ² /s per $\mu\text{g}/\text{m}^3$)	P -value of A_0	Coefficient x_1	P -value of x_1
5	52	0.00211	< 0.001	−0.00017	0.191
5	26	0.00120	< 0.001	−0.0004	0.105
5	14	0.00054	0.004	−0.0001	0.413
5	4	0.00016	< 0.001	−0.00001	0.234
2	13	0.0079	0.0001	−0.0022	0.118
2	6	0.0035	< 0.001	−0.0006	0.146

The observed increase in $d(\Delta P)/c_m/t$ for particles smaller than 0.2 μm is probably due to additional particle deposition by diffusion inside the pores, a mechanism that is expected to be more pronounced with decreasing particle size (Spurny et al. 1969b; Manton 1978).

To better illustrate the dependence of the increase in pressure drop with loading on the filter face velocity (U), the filter pore diameter (D), and particle diameter (d_p), we performed multiple regression of $d(\Delta P)/c_m/t$ on these parameters. This time we included the entire particle size range (i.e., 0.05–2 μm).

Specifically, we expressed $d(\Delta P)/c_m/t$ as follows:

$$\ln\left(\frac{d(\Delta P)}{c_m t}\right)$$
$$= A + x_1 \ln U + x_2 d_p + x_3 \ln D$$

(7)

where A is a constant, and x_1 , x_2 , and x_3 are the coefficients of multiple regression.

The results of this regression are summarized in Table 4. The results of the regression show that the increase in the pressure drop across the filter with loading can be expressed as follows

$$\frac{d(\Delta P)}{c_m t} = 0.0032 \times \frac{U}{D^3 d_p^{0.2}}$$

(8)

In Equation (8), $d(\Delta P)$ is in units of dyn/cm², t in s, c_m in $\mu\text{g}/\text{m}^3$, U in cm/s, and D and d_p are both in μm . A very high correlation coefficient was obtained ($R^2 = 0.98$). This correlation includes the larger particles at high face velocities, for which impaction on the solid filter surfaces tends to decrease the increase in the filter pressure drop with loading. Exclusion of particles larger than 1 μm from this regression increases the value of the correlation coefficient to $R^2 = 0.995$.

Figure 4 shows the measured values of $d(\Delta P)/c_m/t$ plotted against those predicted by the multiple regression model of Equation (8).

TABLE 4. Summary of the multiple regression of the increase in pressure drop per unit time and particle concentration on particle diameter (d_p), filter face velocity (U), and filter pore diameter (D). Multiple regression is based on 51 observations.

	Value	Standard Error	p -value
Constant (A)	−5.74	0.15	10^{-17}
Coefficient of d_p	0.202	0.02	10^{-15}
Coefficient of U	0.996	0.06	10^{-41}
Coefficient of D	−2.978	0.03	10^{-33}
Correlation coefficient R^2	0.98		

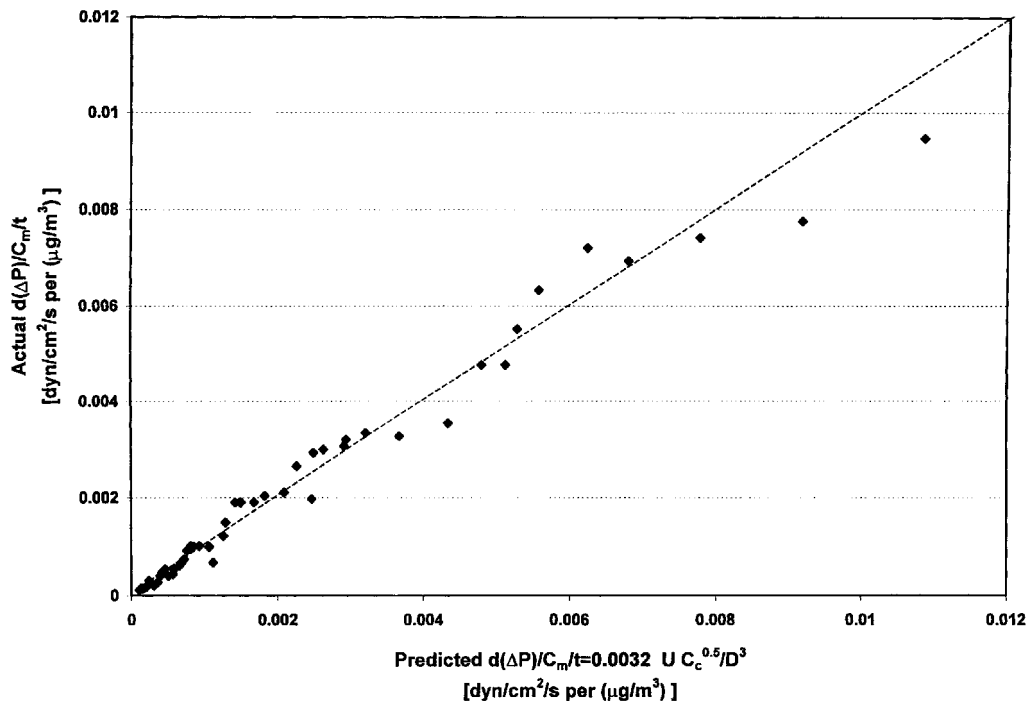


FIGURE 4. Plot of the measured versus model-predicted increase in pressure drop with particle loading.

Figure 4 illustrates the very high correlation between measured and predicted values of the increase in the pressure drop with loading.

A plot of the ratio of the predicted to the actual value of $d(\Delta P)/C_m/t$ as a function of particle Stokes number (St_f), as defined in Equation (4), is shown in Figure 5. The values of the Stokes numbers are plotted in a logarithmic scale so that they are more legible. Figure 5 shows that the measured and predicted values for the pressure drop with loading agree within 20% when the Stokes numbers are smaller than about 5. A sharp increase in the ratio of the predicted to the measured value of $d(\Delta P)/C_m/t$ is observed at St_f values of about 5. Furthermore, the actual value of $d(\Delta P)/C_m/t$ is about 1.5–2 times smaller than the predicted value at St_f values higher than 10. This observation is in remarkable agreement with the theoretical analysis of Smith and Philips (1975). Particles having

Stokes numbers St_f higher than about 5 tend to impact on the solid surface of the Nuclepore filter rather than depositing on the edge of the filter pore, thus they do not contribute to the increase in the pressure drop.

An important implication of Equation (8) is that the pressure drop per mass concentration and time in Nuclepore filters depends rather weakly (to the power of -0.2) on particle size. A possible explanation for this rather weak dependence is that the increase in pressure drop with loading is mostly associated with the reduction in the open pore surface area of the filter. The open pore area of the filter is decreasing over time with particle deposition, hence it should be proportional to the surface area of the depositing particles. Particle deposition onto the pore edges increases with particle size. In contrast, for the same mass loading, smaller particles have a higher overall surface area than larger parti-

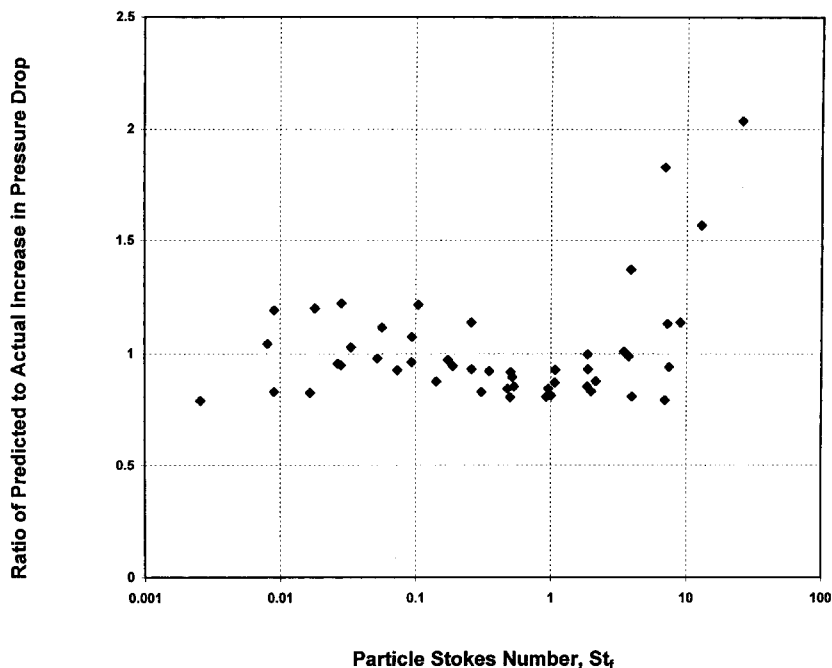


FIGURE 5. Ratio of the predicted to actual increase in pressure drop with particle loading as a function of particle Stokes number.

cles, thus they tend to block more efficiently the surface available to the flow and increase the pressure drop. These effects tend to at least partially cancel each other, thereby rendering the pressure drop weakly dependent of particle size

Effect of Particle Density

The effect of particle density on pressure drop was also investigated in a set of experiments involving monodisperse and polydisperse particles of different densities. Three different densities of particles, including ammonium sulfate ($\rho_p = 1.7 \text{ g/cm}^3$), sodium chloride ($\rho_p = 2.2 \text{ g/cm}^3$) and silica ($\rho_p = 2.6 \text{ g/cm}^3$) were tested. The mass median diameters of the polydisperse sodium chloride and ammonium sulfate aerosols varied from 0.3 to 0.5 μm , as determined with the SMPS/APS monitors. The relative humidity of the test aerosols was controlled in a narrow range of 33–40% for two reasons, 1) to ensure

that the generated particles are dry, and 2) to ensure that the measured value of $d(\Delta P)/C_m/t$ is only a function of particle density and eliminate any effect of the relative humidity (which will be discussed in greater detail in the following section).

The results of the density effect tests are shown in Table 5. Results from these experiments indicated that the pressure drop depends on the inverse of the square root of particle density. The pressure drop (per unit time and mass concentration) was subsequently normalized for the different particle densities, by multiplying by the square root of the particle specific gravity ($s_p = \rho_p/\rho_0$, where ρ_0 is equal to 1 g/cm^3). This normalized pressure drop per unit time and mass concentration (i.e., $d(\Delta P) \cdot (s_p)^{0.5}/C_m/t$) is also shown in the last column in Table 5.

For any face velocity and filter pore configuration, the normalized values show excellent agreement among particles of various densities,

TABLE 5. Density effect on the rate of pressure drop increase as a function of particle mass concentration.

Pore Diameter (μm)	Face Velocity (cm/s)	Particle Type	Particle Size Range ^a (μm)	Density (g/cm^3)	$d(4P)/C_m/t$ ($\times 10^{-3} \text{ dyn/cm}^2/\text{s per } \mu\text{g/m}^3$)	$4P/C_m/t$ (Normalized) ^b ($\times 10^{-3} \text{ dyn/cm}^2/\text{s per } \mu\text{g/m}^3$)
2	13.0	PSL	0.2–1.5	1.05	$7.0(\pm 0.5)$	7.1
		Ammonium sulfate	0.2–1.0	1.7	$5.3(\pm 0.14)$	6.9
		Potassium nitrate	0.2–1.5	2.3	$4.2(\pm 0.14)$	6.4
5	52	PSL	0.2–1.5	1.05	$2.1(\pm 0.14)$	2.2
		Silica	0.5–0.9	2.6	$1.4(\pm 0.07)$	2.3
		Sodium chloride	0.2–1.8	2.2	$1.4(\pm 0.14)$	2.1
	26	PSL	0.2–1.5	1.05	$1.0(\pm 0.07)$	1.02
		Silica	0.5–1.0	2.6	$0.65(\pm 0.06)$	1.05

^a Particle size range is given either the range of diameters of the monodisperse aerosols (PSL) or the range of diameters of the polydisperse aerosols as determined with the SMPS/APS system.

^b Normalized $d(\Delta P)/C_m/t$ is determined by multiplying the value of $d(\Delta P)/C_m/t$ with $s_p^{0.5}$, where s_p is the particle specific gravity.

thereby confirming the dependence of the pressure drop per unit time and mass concentration $d(\Delta P)/C_m/t$ on the square root of particle specific gravity. Hence Equation (8) could be rewritten in the following form in order to incorporate the effect of particle density (or, equivalently, specific gravity):

$$\frac{\Delta P}{c_m t} = 0.0032 \times \frac{U}{s_p^{0.5} D^3 d_p^{0.2}} \quad (9)$$

The expression in Equations (8) and (9) is very similar to the equation describing the pressure drop through an thin orifice for a viscous flow (Happel and Brenner 1975), given by the following equation:

$$\Delta P = K \frac{U \mu}{D^3} \quad (10)$$

where U is the velocity upstream of the orifice, D the diameter of the orifice, and μ the coefficient of viscosity of the fluid. The coefficient K takes values typically in the range 22–24. For Nuclepore filters, the Reynolds number is usually defined as follows (Heidam 1981):

$$\text{Re} = \frac{UD\rho}{\mu p} \quad (11)$$

where U , D , and p are the filter face velocity,

pore diameter, and porosity, respectively; μ and ρ are the air viscosity and density. The Reynolds numbers in all filter configurations that we tested ranged from 0.13 to 1.8, thereby confirming that in any set of experiments, the flow through the pores was viscous.

Effect of Relative Humidity

The increase of the pressure drop per unit time and concentration for ammonium sulfate particles at different relative humidities is shown in Figure 6. A 2- μm pore filter was used, and the filter face velocity was 13 cm/s. The same type of aerosol was used in all of the tests (having a mass median diameter in the range of 0.29–0.32 μm and a geometric standard deviation varying from 1.9–2.3). The experimental results in Figure 6 show a very strong dependence of $d(\Delta P)/c_m \cdot t$ on the relative humidity. The value of $d(\Delta P)/c_m \cdot t$ nearly doubles as the relative humidity decreases from the 30–38% range to 10–15% (from 0.005 to about 0.01 $\text{dyn/cm}^2/\text{s per } \mu\text{g/m}^3$). Since ammonium sulfate particles are dry in these ranges of RH, the increase in the pressure drop with loading could not be due to altering the physical characteristics of the particles. A possible explanation for this increase of pressure drop with loading at lower

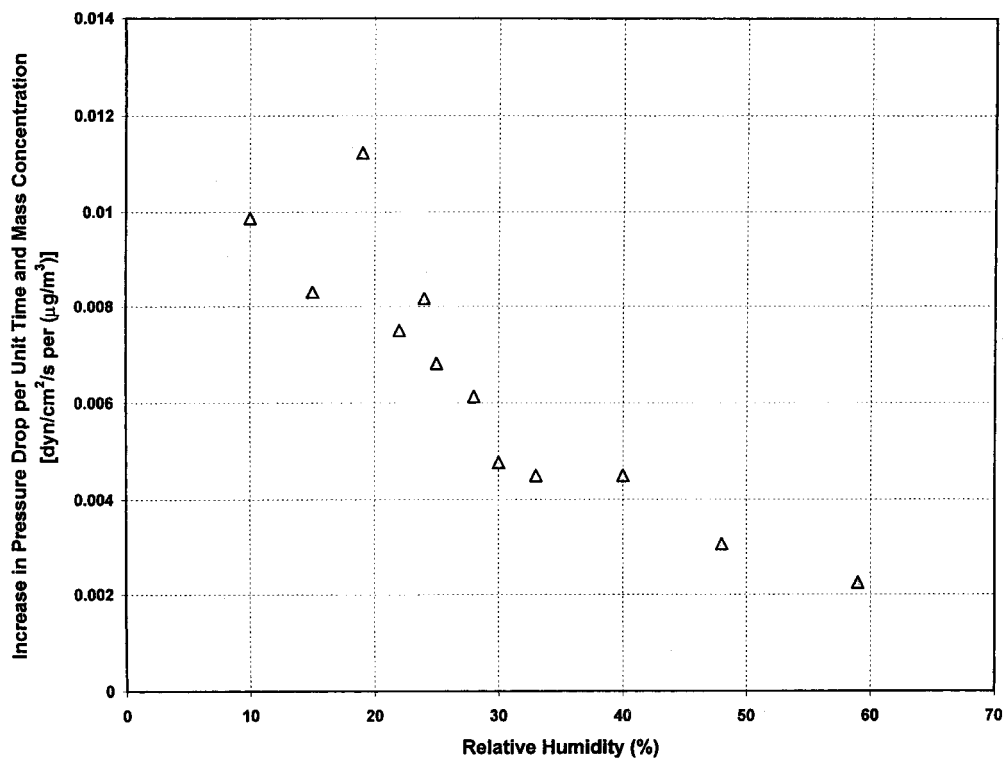


FIGURE 6. Pressure drop with particle loading as a function of relative humidity. Ammonium sulfate was particles used as the test aerosol.

RH may be an increase in particle deposition due to electrostatic mechanisms, which would be more prominent at lower relative humidities.

Increasing further the RH to values above 40% also results in a decrease in pressure drop per unit concentration and time, but not as sharp as that observed for the lower RH ranges. The average value of $d(\Delta P)_{c_m} \cdot t$ decreases to about 0.002 from 0.005 dyn/cm²/s per $\mu\text{g}/\text{m}^3$ (corresponding to RH in the range 33–39%). This further decrease reflects the difference in the response of Nuclepore filters with particle loading when liquid instead of solid particles are used. Although the deliquescence point of pure ammonium sulfate is 80% (Tang 1976), the $(\text{NH}_4)_2\text{SO}_4$ particles generated in our tests by a nebulizer are initially liquid droplets which are dried by being mixed with clean air of adjustable RH. These droplets become completely dry at

RH values below 40%, hence at higher values, the particles collected by the Nuclepore filter may be in the form of droplets.

A similar decrease in pressure drop with particle loading has been observed in HEPA filters by Gupta et al. (1993). When hygroscopic sodium chloride particles were used, the pressure drop per unit mass of particle loading nearly doubled as the relative humidity decreased from 55 to 35%. Since the mechanisms responsible for increasing the pressure drop in HEPA filters may be somewhat different to those in Nuclepore, this similar behavior may be incidental.

CONCLUSIONS

This experimental study investigated the relationship between the increase in pressure drop with particle loading in Nuclepore filters and

particle size, as well as filter design and operating parameters. The average increase in pressure drop per unit time and particle mass concentration was measured as a function of particle size, density, and hygroscopicity. Two different Nuclepore filter pore diameters were tested (2 and 5 μm , respectively) at filter face velocities ranging from 4 to 52 cm/s.

Our results showed that the increase in the pressure drop with particle loading is inversely proportional to the square root of particle density and depends weakly on particle size (to the power of -0.2). Particle interception and impaction on the pore edges are the main deposition mechanisms that are responsible for raising the pressure drop over time across the filter, especially for particles having Stokes numbers below 5. This observation agrees well with previously published studies on particle deposition on the pore edges in Nuclepore filters. Our tests also showed a dramatic decrease in the pressure drop with loading for hygroscopic particles as the relative humidity increases from 10 to 50%. The pressure drop with loading decreases almost inversely proportional to the relative humidity for ammonium sulfate particles.

Based on the experimental results, the increase in pressure drop with particle loading in Nuclepore filters could be used to measure particle concentration when particle density and size are known, at a given relative humidity. These conditions could be achieved in laboratory experiments. Further, the effect of relative humidity cannot be ignored. Although it is possible to control the relative humidity of the sampled aerosol within a 5–10% range, this may make the method expensive and complicated, thereby depriving it of its simplicity. Therefore this technique will yield problematic results if used in an environment where ambient relative humidity cannot be accurately controlled.

References

- Fan, K. C., Leaseburge, C., Huyn, Y., and Gentry, J. (1978). Clogging in Nuclepore Filters; Cap Formation Model, *Atmos. Environ.* 12:1797–1802.
- Gupta, A., Novick, V. J., Biswas, P., and Monson, P. R. (1993). Effect of Humidity and Particle Hygroscopicity on the Mass Loading Capacity of High Efficiency Particulate Air (HEPA) Filters, *Aerosol Sci. and Technol.* 19:94–107.
- Happel, J., and Brenner, H. (1975). *Low Reynolds Number Hydrodynamics*, Edgwood Cliffs, N.J., Prentice Hall, Inc.
- Heidam, N. Z., (1981). Review: Aerosol Fractionation by Sequential Filtration with Nuclepore Filters, *Atmos. Environ.* 15:891–904.
- Koutrakis, P., Wang, P.Y., Wolfson, J.M., and Sioutas, C. (1995). Continuous Monitor to Measure Particulate Matter in Gas: Patent filed by Harvard University. U.S. Patent No. 5,571,945.
- Manton, M. J. (1978). The Impaction of Aerosols on a Nuclepore Filter, *Atmos. Environ.* 12:1669–1675.
- Muysshondt, A., McFarland, A. R., and Anand, N. K. (1996). Deposition of Aerosol Particles in Contraction Fittings, *Aerosol Sci. and Technol.* 24:205–216.
- Pich, J. (1964). Impaction of Aerosol Particles in the Neighborhood of a Circular Hole, *Colln. Czech. Chem. Commun.* 29:2223–2227.
- Smith, T. N., and Phillips, C. R. (1975). Inertial Collection of Aerosol Particles at Circular Aperture, *Environ. Sci. and Technol.* 9:564–568.
- Spurny, K., Lodge, J. P., Frank, E. R., and Sheesley, D. C. (1969a). Aerosol Filtration by Means of Nuclepore Filters: Structural and Filtration Properties, *Environ. Sci. and Technol.* 3:453–464.
- Spurny, K., Lodge, J. P., Frank, E. R., and Sheesley, D.C. (1969b). Aerosol Filtration by Means of Nuclepore Filters: Aerosol Sampling and Measurement, *Environ. Sci. and Technol.* 3:464–468.
- Tan, I. N. (1976). Phase Transformation and Growth of Aerosol Particles composed of mixed salts. *J. Aerosol Sci.* 7:361–371.
- Wang, P.Y., (1997). *Continuous Aerosol Mass Measurement by Flow Obstruction*. S.D. Thesis, Harvard University, School of Public Health, Boston, MA.
- Ye, Y., and Pui, D. Y. H. (1990). Particle Deposition in a Tube with an Abrupt Contraction. *J. Aerosol Sci.* 21:29–40.